https://doi.org/10.5194/egusphere-2026-4934
Preprint. Discussion started: 21 September 2026

Technical note: Development and field validation of SMART-ASF, a low-cost automated soil gas flux monitoring system for long-term field observations

Ching-Chou Fu[1,*], Sheng-Fu Hu[2], Li-Hung Lin[3], Kuo-Hang Chen[1], Chin-Shang Ku[1], Hao Kuo-Chen[3], Kuo-Wei Wu[1], Chin-Jen Lin[1]

1. Institute of Earth Sciences, Academia Sinica, Taiwan
2. XY ELECCONTROL TECHNOLOGY CO., LTD, Taoyuan, Taiwan
3. Department of Geosciences, National Taiwan University, Taipei, Taiwan

*.**Corresponding author**: Ching-Chou Fu
Institute of Earth Sciences, Academia Sinica, Taiwan
E-mail: ccfu@earth.sinica.edu.tw
Tel.: +886-2-2783-9910 ext.1513
Fax: +886-2-2783-9871

https://doi.org/10.5194/egusphere-2026-4934
Preprint. Discussion started: 21 September 2026

Abstract

Continuous, high temporal resolution measurements of soil gas fluxes are essential for understanding terrestrial carbon cycling and subsurface fluid processes, yet long-term autonomous monitoring remains limited by the high cost and operational complexity of conventional systems. This study presents the development and field validation of the SMART Automated Soil Flux (SMART-ASF) system, a low-cost and modular platform that integrates automated chamber-based flux measurements, low-cost gas sensing, wireless telemetry, and solar powered autonomous operation for continuous soil CO_2 flux monitoring.

Laboratory calibration against a commercial LGR M-GGA-918 analyzer demonstrated excellent linearity ($R^2 \approx 1$) over a CO_2 concentration range of approximately 100 to 8500 ppm, with relative deviations generally within 3 to 5 % over the concentration range most relevant to soil gas flux measurements. Independent comparisons with conventional manual closed chamber measurements showed good agreement under field conditions. Long-term field deployment for more than five months demonstrated stable unattended operation without routine maintenance or component replacement under natural environmental conditions. Continuous observations successfully captured both short-term and seasonal variations in soil CO_2 flux, including a marked suppression of emissions during intense rainfall associated with Typhoon Fengshen and the subsequent recovery of background fluxes. The system also consistently resolved low background fluxes below 0.1 g m^{-2} d^{-1}, demonstrating sufficient sensitivity for monitoring low emission environments.

These results support the applicability of the SMART-ASF system for long-term automated soil gas flux monitoring and its potential use in terrestrial carbon cycle research and environmental geochemical monitoring.

Keywords: automated soil flux system; soil CO_2 flux; low-cost sensor; continuous monitoring; terrestrial carbon cycling

https://doi.org/10.5194/egusphere-2026-4934
Preprint. Discussion started: 21 September 2026

1. Introduction

Gas exchange at the soil–atmosphere interface is a central process in the terrestrial carbon cycle and within the Critical Zone, where microbial respiration, root activity, and abiotic reactions collectively regulate CO_2 fluxes. These fluxes reflect the biogeochemical dynamics of soils and play a crucial role in evaluating global greenhouse gas budgets and climate feedbacks (e.g., Holland et al., 1999; Werner et al., 2007). High frequency measurements obtained from automated closed chambers coupled with online analyzers have demonstrated the capability to continuously resolve instantaneous fluxes and diel variability of CO_2, CH_4, and N_2O under field conditions. This approach substantially improves the detection of short-term and event driven variations that are often missed by manual sampling (Savage et al., 2014; O'Connell et al., 2018).

Compared with the eddy covariance technique (Aubinet et al., 1999; Aguilos et al., 2018), chamber-based methods provide finer spatial resolution and are particularly suitable for heterogeneous terrain and complex environmental settings. Automated non steady state chamber systems further enable high frequency flux measurements, efficient processing of large datasets, and temporal upscaling, making them widely adopted for long-term ecosystem monitoring (Livingston et al., 2005; Courtois et al., 2019; Themistokleous et al., 2024).

Beyond ecological applications, soil gas fluxes also serve as sensitive indicators of geological activity. Along active faults and volcanic systems, deep sourced fluids migrate through permeable structures and produce temporal and spatial anomalies in soil CO_2 fluxes together with other tracers such as radon and helium (Chiodini et al., 2008; Yuce et al., 2017; D'Alessandro et al., 2020; Li et al., 2024; Fu et al., 2025). Continuous soil gas monitoring therefore provides valuable information for investigating fluid migration, fault permeability, volcanic degassing, and earthquake related processes (Fu et al., 2017; Girault et al., 2018).

Recent advances in automated chamber systems have focused on improving temporal resolution, reducing system cost, and increasing operational autonomy through low-cost sensors, open source electronics, and wireless communication technologies (Bastviken et al., 2015, 2020; Blackstock et al., 2019; Brown et al., 2020; Forbes et al., 2023; Macagga et al., 2024; Zawilski and Bustillo, 2024; Tonolo et al., 2025). These developments have substantially expanded the feasibility of long-term field observations and dense monitoring networks. Nevertheless, many existing systems

https://doi.org/10.5194/egusphere-2026-4934
Preprint. Discussion started: 21 September 2026

still rely on relatively expensive analyzers, complex mechanical structures, or limited sensor integration, which constrain their scalability and widespread deployment, particularly in remote environments. Furthermore, relatively few systems simultaneously integrate automated chamber measurements, expandable multi gas capability, wireless cloud-based data transmission, autonomous power management, and long-term unattended operation into a single monitoring platform.

The present study is motivated by three interrelated needs. First, high temporal resolution and long-term continuous soil gas flux measurements are required to capture event driven processes, such as rainfall induced degassing, and to provide reliable surface observations relevant to fault activity and earthquake fluid interactions. Second, there is a need for a modular and low-cost system architecture that enables scalable deployment and improved spatial coverage while maintaining measurement performance. Third, long-term autonomous operation under remote environmental conditions requires robust integration of sensing, power management, wireless communication, and real time data visualization.

To address these needs, we developed SMART-ASF (Smart Monitoring and Automated Real Time system coupled with an Automated Soil Flux module), in which the ASF module serves as the core component for continuous soil gas flux measurements. The system integrates automated closed chamber measurements, low-cost gas sensing with expandable multi gas capability, intelligent gas circulation, cloud-based data management, and solar powered autonomous operation. This technical note describes the design, calibration, field validation, and long-term deployment of the SMART-ASF system and evaluates its performance for continuous soil CO_2 flux monitoring under natural field conditions.

2. Methods

2.1 Composition and Operating Principles of the Gas Flux Monitoring System

This study developed the SMART-ASF system, in which the Automated Soil Flux (ASF) module enables long-term, continuous, real-time, and high-frequency soil gas flux monitoring. The SMART-ASF architecture comprises four major components: (1) ASF Sensor Unit (ASF-SU), which integrates multiple gas and temperature sensors, a control unit, a diaphragm pump, and data storage; (2) ASF Gateway Unit (ASF-GW), which includes a control module, wireless communication module, and expandable temperature sensing modules; (3) Power supply, composed of lithium battery packs in

https://doi.org/10.5194/egusphere-2026-4934
Preprint. Discussion started: 21 September 2026

conjunction with a solar power system, including a battery voltage monitor Unit for real-time voltage tracking; and (4) Closed chamber, which serves as the gas accumulation and measurement enclosure.

2.2 System Architecture and Components

Within the ASF-SU, the gas sensing module is housed inside a dedicated sensor chamber. This chamber is equipped with sensors for carbon dioxide (0-4%; Senseair K30), sulfur dioxide (0-1000 ppm; EC Sense ES4-SO2-1000), and hydrogen sulfide (0-500 ppm; EC Sense ES4-H2S-500). The sensor modules are individually replaceable and can be readily exchanged or expanded with additional gas sensors according to specific monitoring objectives, providing a flexible and modular platform for future system upgrades. The sensing chamber also integrates a barometric pressure sensor (BMP280, BOSCH) and a temperature-humidity sensor (SHT31) to monitor internal environmental conditions. The operating ranges and accuracies are as follows: pressure range 300 to 1100 hPa with an accuracy of ±0.12 hPa; temperature range −40 to 125 °C with an accuracy of ±0.3 °C; and relative humidity range 0 to 100% with an accuracy of ±2%.

A custom developed Xy_SensorBOX, implemented in house for this study, is used as the central control and data processing unit of the system. The unit is based on a microcontroller (Arm®Cortex®-M0 32-bit RISC core) architecture and provides integrated functions for data acquisition, system control, and communication. It manages the operation schedule of the brushless diaphragm pump (PZX512BL; Ever Motor Guanlian Corp., Taiwan), which has a rated flow capacity of approximately 4–7 L min^{-1} at 12 V DC. The pump output is software configurable, allowing the operating flow rate to be adjusted according to system requirements. The pump is capable of continuous operation with a service lifetime exceeding one year. The system further incorporates a Nafion-based gas drying module (Perma Pure Co.) to regulate moisture in the gas stream, onboard data storage via a MicroSD card (up to 32GB, Kingston), wireless data transmission through a Wi-Fi interface, and a solar powered energy supply to enable long-term autonomous field deployment. Detailed hardware specifications and operational parameters of the Xy_SensorBOX are provided in the Supplementary Fig. S1.

A polypropylene (PP) enclosure with external dimensions of 200 mm × 200 mm × 130 mm was used to house the system components. The components summarized in

https://doi.org/10.5194/egusphere-2026-4934
Preprint. Discussion started: 21 September 2026

Supplementary Table S1 were securely mounted within the enclosure using a mold-based positioning approach designed to minimize pump induced vibrations and improve overall system stability.

The ASF_GW was housed in a polypropylene enclosure with external dimensions of 100 mm × 100 mm × 40 mm. The unit integrates a WiFi communication module (ESP32-WROOM-32E-H4) and a custom developed Xy_SensorBOX microcomputer, which functions as the central control and data processing unit of the system. Two temperature sensors (SHT31) are connected via an RS485 interface and enclosed within stainless steel pipes to ensure sealed protection for subsurface soil temperature measurements. The overall system architecture and component configuration of the ASF module are illustrated in Figure 1.

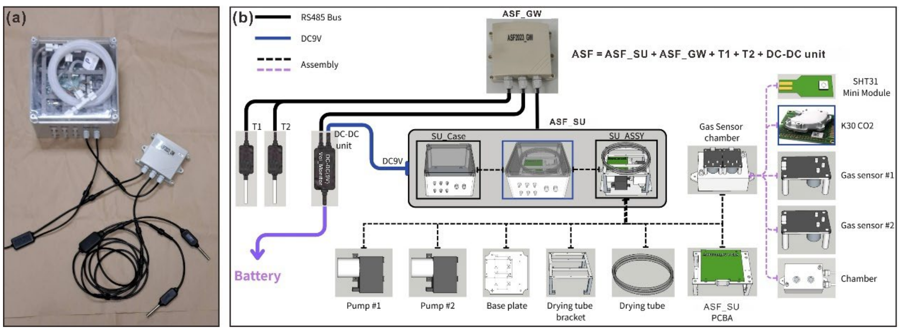

Figure 1. Block diagram illustrating the configuration and functional connections of the Automated Soil Flux (ASF) module. The ASF consists of the gateway unit (ASF_GW), sensor unit (ASF_SU), two soil temperature sensors (T1 and T2), a DC–DC converter unit with integrated voltage monitor and RS-485 interface, and a battery supply input port. The diagram shows the integrated connections among major components, including the gas sensor chamber, dual pumps, drying tube assembly, and the CO_2 (K30) and SHT31 sensors, highlighting the coordinated operation of power delivery, data communication, and gas flow control within the system.

2.3 Measurement Method and Gas Circulation Process

Soil gas flux was determined using a closed chamber method. The closed chamber consisted of a cylindrical enclosure with a diameter of 20 cm and a height of 40 cm (base area 314 cm²), constructed from polyvinyl chloride (PVC). The dimensions of the closed chamber are configurable and can be adjusted according to specific monitoring requirements; under high flux conditions, a larger chamber volume may be adopted to

https://doi.org/10.5194/egusphere-2026-4934
Preprint. Discussion started: 21 September 2026

accommodate elevated gas emission rates. In the present study, an opaque PVC chamber was selected because the primary objective was continuous monitoring of soil gas emissions rather than ecosystem carbon exchange. For ecological applications requiring measurements of vegetation–atmosphere CO_2 exchange, the chamber can be readily fabricated from transparent acrylic to allow natural light penetration while retaining the same measurement principle (e.g., Savage et al., 2014). The base was filled with approximately 20 cm of fine-grained quartz sand to provide a stable and homogeneous substrate, thereby minimizing variability associated with vegetation growth, root respiration, and other near-surface biological processes during long-term field deployment. This configuration provided a stable substrate for long-term in situ measurements. The effective internal gas volume was approximately 6000 cm^3 (Figure 2). The system included two diaphragm pumps with operational flow rates set at ~1 L min^{-1} and ~2 L min^{-1}, respectively, to optimize gas circulation and chamber flushing during the measurement cycle.

The first pump continuously directed the air from the chamber into the sensor housing for gas concentration analysis. A particulate filter was installed at the inlet to prevent dust from entering the system. After analysis, the gas was returned to the closed chamber through four directional outlets that generated uniform turbulence, ensuring complete gas mixing and repeated circulation for analysis (Fu et al., 2025). Gas mixing within the chamber was achieved without an internal fan, thereby reducing the number of moving components and the mechanical complexity of the system. A one-way vent valve was incorporated into the chamber to minimize pressure buildup during both the accumulation and flushing stages. By maintaining chamber pressure close to ambient conditions, the valve helps reduce potential pressure induced suppression of soil gas diffusion and minimizes feedback effects associated with progressive CO_2 accumulation. As illustrated in Figure 3, CO_2 concentrations increased approximately linearly throughout the selected measurement interval while chamber pressure and internal temperature remained nearly constant. These observations indicate stable chamber conditions during flux measurements and suggest that significant chamber-related artifacts, including pressure-induced suppression of soil gas diffusion and nonlinear feedback associated with progressive CO_2 accumulation, were not evident under the operating conditions adopted in this study.

The second pump was activated after each flux determination to introduce fresh air into the closed chamber. It operated at a flow rate of ~2 L min^{-1} for 10 minutes,

https://doi.org/10.5194/egusphere-2026-4934
Preprint. Discussion started: 21 September 2026

flushing the chamber through a one-way valve and achieving at least 3 complete air exchanges. This process restored gas concentrations to background levels before the next measurement cycle. This flushing procedure reproduced the gas-renewal function of an automated open–close chamber without requiring a mechanically actuated chamber lid. To prevent condensation within the tubing and maintain sensor stability during prolonged measurements, a Nafion drying tube was incorporated for dehumidification. The pressure gradient across the Nafion membrane continuously removed water vapor from the sampled gas stream, reducing condensation and humidity-related interference. Although alternative drying materials or desiccators could also be used, their potential background contribution, gas adsorption characteristics, and possible influence on the measured gas composition should be evaluated prior to deployment to ensure measurement accuracy.

Additionally, two temperature probes were installed adjacent to the chamber at depths of 20 cm (T_{S20}) and 100 cm (T_{S100}) below the soil surface to enable continuous monitoring of vertical soil temperature variations. The SMART-ASF system was deployed at a permanent field observation site on the campus of Academia Sinica, Taipei, Taiwan (25.0402° N, 121.6123° E), established for long-term soil gas monitoring. Figure 2 illustrates the field deployment configuration of the SMART-ASF system at the observation site.

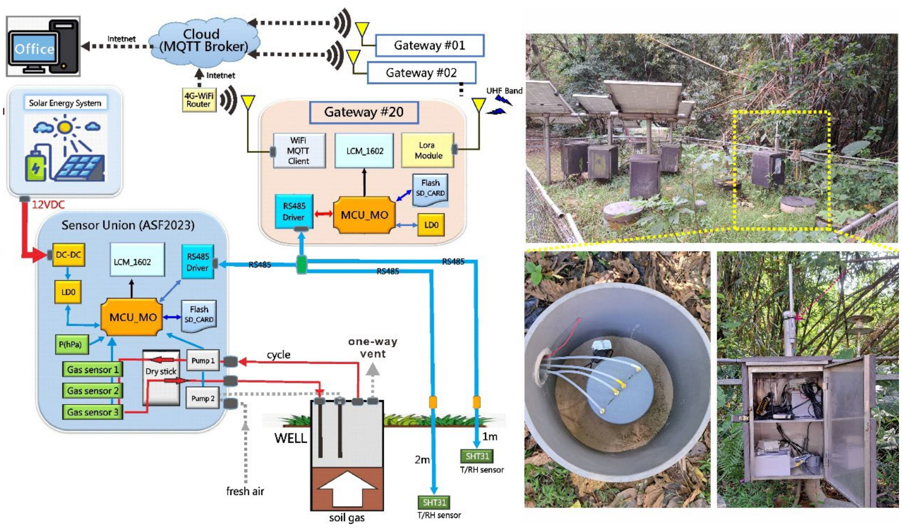

Figure 2. Field deployment schematic of the SMART-ASF system, illustrating the integration of power supply, sensor unit, gateway, and wireless data transmission to a cloud-based MQTT platform. Soil gas flux is measured using a closed chamber coupled

https://doi.org/10.5194/egusphere-2026-4934
Preprint. Discussion started: 21 September 2026

with a dual pump circulation and flushing system, enabling efficient gas mixing without internal fans and automated restoration to background conditions. Additional soil temperature sensors installed at depths of 20 cm and 100 cm provide complementary subsurface thermal observations, supporting long-term unattended monitoring.

2.4 Data Acquisition and Flux Calculation

The automated soil gas flux system in this study recorded continuous data at 10-second intervals, which could be adjusted according to research requirements. The monitored parameters included the CO_2 concentration, temperature, and air pressure within the closed chamber, soil temperature at different depths, and system voltage. Each measurement cycle lasted approximately 50 minutes, providing sufficient CO_2 concentration data for flux calculation. The concentration variation exhibited a distinct linear increase trend during the measurement period (as shown in Figure 3, pink-shaded area representing the measurement period). Upon completion of each measurement, the second pump was activated to perform gas flushing, replacing the chamber air with background air (as shown in Figure 3, gray-shaded area representing the flush gas period) to restore the concentration to baseline before initiating the next cycle.

However, observations revealed that at the onset of flushing, CO_2 concentration did not decrease immediately but continued to rise for approximately 2 minutes. Conversely, when flushing ceased, CO_2 concentration continued to decrease for an additional approximately 2 minutes before reaching stability. This time lag indicates a delayed concentration response, likely reflecting the combined effects of gas transport through the chamber–tubing system, chamber mixing, sensor response time, and the efficiency of gas exchange. At the beginning of the flushing stage, residual high-concentration gas within the circulation pathway was progressively displaced rather than instantaneously replaced, while CO_2 concentrations inside the chamber also required finite time to decrease. Conversely, after flushing ceased, low-concentration air remaining within the circulation pathway required additional time to be replaced by newly accumulated soil gas. This delayed response phenomenon was defined in this study as the “delay zone”, as indicated by the red hatched region in Figure 3.

Because the gas within the closed chamber required approximately 5 minutes after flushing to achieve a stable mixing condition and begin accumulating CO_2 again, only the steady and linear portion of the CO_2 concentration increase (from the 10th to the 45th minute) in each measurement cycle was selected for flux calculation. The CO_2 flux

https://doi.org/10.5194/egusphere-2026-4934
Preprint. Discussion started: 21 September 2026

was calculated using the closed chamber method described by Chiodini et al. (1998), with an estimated system uncertainty of approximately 10%. The calculation was based on the rate of CO_2 concentration increase (dc/dt) within the chamber, combined with the mean pressure and temperature during the same period, to obtain the soil CO_2 flux (F_{CO_2}, g m^{-2} d^{-1}). The flux was calculated according to the following equation:

$$F_{CO2} = k\frac{P\,V}{S\,T}\frac{dc}{dt} \quad (1)$$

where k is the gas constant, P is atmospheric pressure (Pa), V is the volume of the chamber (m³), S is the base area of the chamber (m²), and T is soil temperature (K). In this system, the soil temperature at a depth of 20 cm (T_{S20}) was used in the calculation.

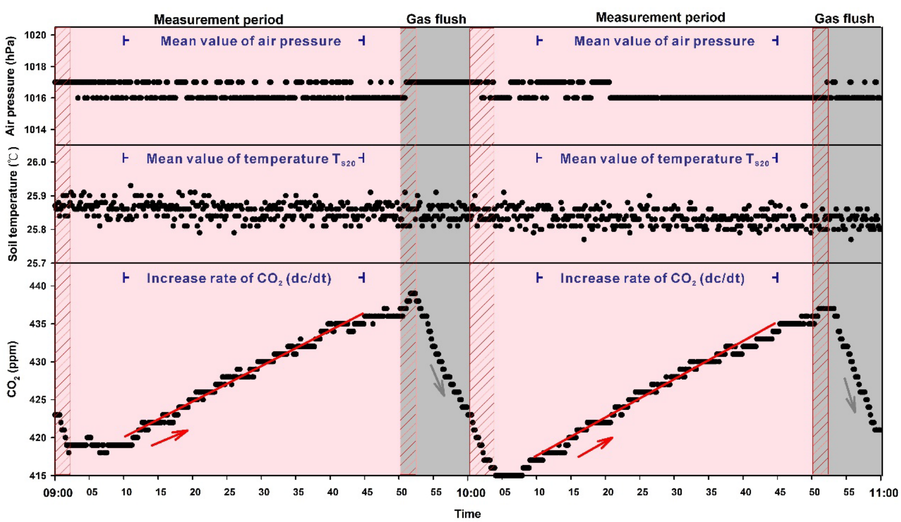

Figure 3. Time series of air pressure, soil temperature, and CO_2 concentration during automated flux measurements. The pink areas indicate measurement periods with linear CO_2 increase used for flux calculation, the gray areas represent gas flushing, and the red hatched zones mark delay intervals caused by transient gas mixing within the chamber system after the switch of pumping.

2.5 Data Transmission and Remote Monitoring

Data transmission in the SMART-ASF system was managed through the ASF-GW, which retrieved data from the ASF-SU at scheduled intervals of 10 seconds. The collected monitoring data were simultaneously transmitted in real time to a cloud server (MQTT broker) through the built-in Wi-Fi, while a laboratory host server received synchronized copies of the data for integration and visualization.

https://doi.org/10.5194/egusphere-2026-4934
Preprint. Discussion started: 21 September 2026

Data visualization and monitoring were performed using the open-source platform Grafana (https://grafana.com), which is characterized by its high modularity and interactivity. Grafana enables real-time access to various databases such as MQTT and MySQL, displaying monitoring parameters through dynamic and customizable dashboards. Users can configure the visualization time scale, refresh frequency, and alert thresholds, as well as conduct cross-sensor data comparisons and trend analyses (Figure 4).

If the ASF-GW fails to obtain data from the ASF-SU for more than 10 minutes, the system automatically transmits a "No data" alert message to indicate a potential malfunction. Additionally, the ASF-GW is programmed to reboot daily at 00:00 to maintain system stability and ensure smooth network performance by clearing potential communication errors.

Figure 4. Time series of a 12 hour continuous observation acquired by the SMART-ASF system and visualized using Grafana, showing synchronized measurements of chamber gas concentrations, temperature, humidity, soil parameters, atmospheric pressure, and system voltage. Data were recorded at 10 second intervals and transmitted in real time to cloud and laboratory servers.

2.6 Power Supply and System Stability

The SMART-ASF system operates at a nominal voltage of 5 V, while the air pumps are powered at 9 V. An integrated DC–DC converter allows the system to accept a DC input voltage ranging from 4 to 18 V. Depending on field conditions, the system can be powered either by AC mains electricity through an appropriate power adapter or

https://doi.org/10.5194/egusphere-2026-4934
Preprint. Discussion started: 21 September 2026

by a battery pack. Power consumption of the ASF unit was evaluated using an INA226 power-monitoring chip. The 24 h power profile shown in Figure 5 indicates an average power consumption of approximately 2.84 W, with a baseline of approximately 2.2 W and hourly increases associated with the chamber-flushing cycle, during which power consumption reached a maximum of approximately 6.23 W. The brief decrease to approximately 0.47 W near midnight corresponds to the scheduled automatic system restart and represents a normal part of the operating cycle rather than a power interruption. The communication infrastructure, including Wi-Fi and 4G telemetry, consumed an additional approximately 2.1 W, resulting in an estimated total average system power consumption of approximately 4.94 W.

In this study, the SMART-ASF system was primarily powered by a 14.4 V lithium-ion battery pack (Samsung INR21700-50E, 4S13P configuration, total capacity 63.7 Ah), integrated with a 300 W solar photovoltaic module and a solar charge controller (Morningstar PS-15M). The nominal battery capacity corresponds to approximately 917 Wh, providing a theoretical operating duration of approximately 7.7 d at the estimated average system power consumption of 4.94 W in the absence of solar charging. This estimate is consistent with field observations showing that the system could operate on battery power for approximately one week during prolonged periods of low solar radiation. No routine maintenance of the power module was required during the field deployment period of more than five months.

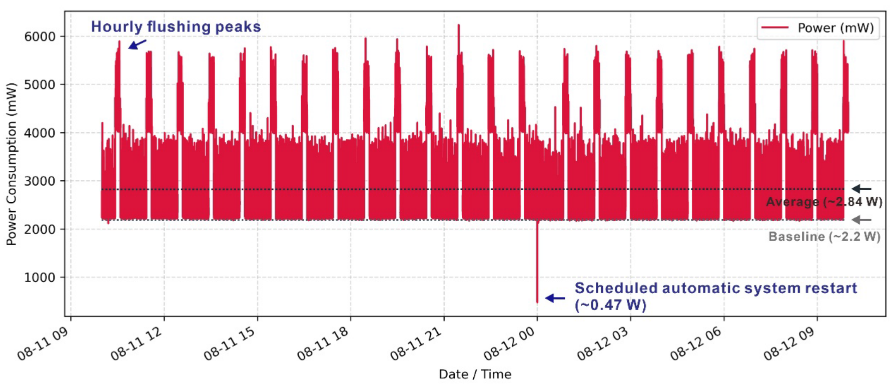

Figure 5. Twenty-four-hour power consumption profile of the ASF unit measured using an INA226 power-monitoring chip. The baseline power consumption was approximately 2.2 W, with hourly increases associated with the chamber-flushing cycle and a maximum instantaneous power consumption of approximately 6.23 W. The average power consumption over the 24 h measurement period was approximately 2.84

https://doi.org/10.5194/egusphere-2026-4934
Preprint. Discussion started: 21 September 2026

W. The brief decrease to approximately 0.47 W near midnight corresponds to the scheduled automatic system restart.

3. Results and Discussion

3.1 Laboratory validation and performance evaluation

Figure 6a illustrates the comparative relationship between CO_2 concentrations measured by the K30 sensor employed in this study and those obtained using the commercial LGR-ICOS gas analyzer (M-GGA-918). Prior to the comparison experiment, the K30 sensor was calibrated using certified standard gases over a CO_2 concentration range of approximately 100–8500 ppm, encompassing the concentrations typically encountered during automated soil gas flux measurements. The calibrated K30 sensor was subsequently evaluated against the LGR M-GGA-918, which served as the reference instrument for independent performance validation. The experimental setup involved connecting both the ASF module and the LGR M-GGA-918 to the same gas chamber, which was initially filled with zero air and subsequently injected with CO_2 of increasing concentrations to establish a series of controlled CO_2 concentration levels. The results show an excellent linear correlation between the two instruments ($R^2 \approx 1$), with the regression equation $y = 1.05x - 6.5$. The calibration covered CO_2 concentrations from approximately 100 to 8500 ppm, encompassing the concentration range typically encountered during automated soil gas flux measurements under natural field conditions. The slope being slightly greater than unity indicates a minor overestimation by the K30 at higher concentrations (>6000 ppm); however, the overall deviation remains negligible, and the regression line nearly coincides with the ideal 1:1 reference line.

This finding demonstrates that the K30 sensor exhibits a linear response across a wide range of CO_2 concentrations, accurately capturing concentration variations. Compared with the LGR M-GGA-918, the K30 achieves excellent agreement when properly calibrated and operated under stable airflow conditions, with deviations remaining within only a few percent throughout the evaluated concentration range. Such linearity improves confidence in subsequent field measurements for long-term field applications (Brown et al., 2020; Forbes et al., 2023). Although the comparison was conducted under controlled laboratory conditions, the calibrated K30 achieved analytical performance comparable to the LGR analyzer over the evaluated concentration range, supporting its subsequent field application.

https://doi.org/10.5194/egusphere-2026-4934
Preprint. Discussion started: 21 September 2026

Figure 6b presents the results of the same experimental setup, showing the CO_2 concentrations and relative percentage differences measured by the K30 sensor and the LGR M-GGA-918 across a series of controlled concentration levels. Each dataset represents a steady-state condition within the chamber at a specific CO_2 concentration, with red symbols corresponding to K30 measurements and black symbols to LGR readings. The concentration trends of both instruments are highly consistent, and the relative deviations remain within ±8% across the entire concentration range. Specifically, relative deviations were approximately 8% below 200 ppm, decreased to 3–4% over the 400–2000 ppm range, and remained around 5% at higher concentrations.

The slightly larger deviation at very low concentrations is consistent with the reduced signal-to-noise ratio of NDIR sensors under low-signal conditions. Across the concentration range most relevant to soil gas monitoring, the calibrated K30 achieved analytical performance comparable to that reported for other low-cost NDIR systems and approached that of the LGR M-GGA-918 analyzer (Bastviken et al., 2015; Brown et al., 2020; Macagga et al., 2024). These findings indicate that calibrated low-cost NDIR sensors can substantially reduce the cost of long-term automated monitoring systems while maintaining analytical performance comparable to laboratory-grade instruments.

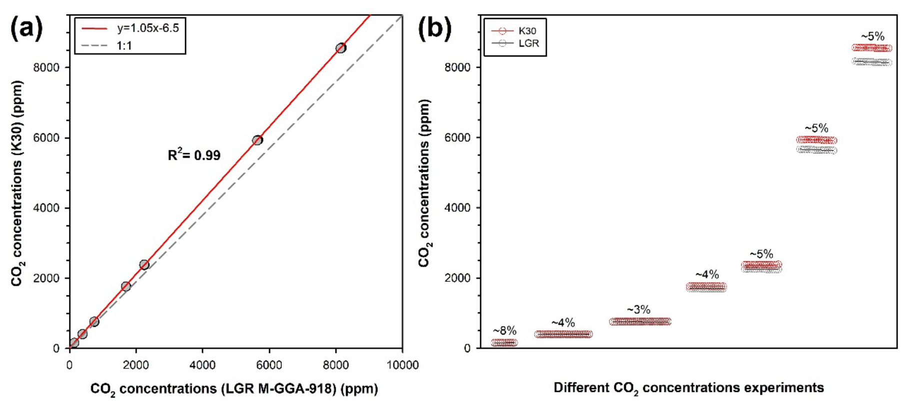

Figure 6. Laboratory validation of the CO_2 sensing performance of the SMART-ASF system. (a) Calibration relationship between the K30 nondispersive infrared sensor and the commercial LGR M-GGA-918 analyzer over the concentration range of approximately 100 to 8500 ppm. The dashed line represents the ideal 1:1 relationship. (b) Measured CO_2 concentrations at individual calibration levels together with the corresponding relative deviations between the two instruments.

https://doi.org/10.5194/egusphere-2026-4934
Preprint. Discussion started: 21 September 2026

To further validate the performance of the complete SMART-ASF system, automated CO_2 flux measurements were compared with independent manual closed chamber measurements conducted on multiple occasions following the protocol described by Fu et al. (2025). The comparisons included measurements at the permanent SMART-ASF observation site under background flux conditions and at a nearby temporary site established to evaluate higher CO_2 fluxes. Figure 7a summarizes the relationship between paired SMART-ASF and manual chamber measurements over a broad range of CO_2 fluxes, encompassing both background and elevated emission conditions. Excellent agreement was obtained between the two methods (R^2 = 0.99, n = 19), with the regression line closely following the 1:1 reference line, indicating that the automated measurements closely reproduced manually determined CO_2 fluxes under natural field conditions over a wide range of CO_2 fluxes spanning approximately 0.1 to 5.4 g m^{-2} d^{-1}. This validated range encompasses typical background as well as elevated soil CO_2 emissions encountered in many environmental and geological monitoring applications, supporting the applicability of the SMART-ASF system across diverse field conditions.

Figures 7b and 7c further compare paired measurements as a function of measurement time under relatively low- and high-flux conditions, respectively. In both cases, the SMART-ASF system consistently captured the temporal variations observed by the conventional manual chamber method, demonstrating that the automated chamber measurements faithfully reproduced the overall pattern of CO_2 flux variability. Although the SMART-ASF measurements exhibited a slight systematic underestimation relative to the manual measurements, the discrepancy remained consistent across both flux regimes, suggesting that the observed differences primarily reflect a systematic proportional bias rather than flux-dependent measurement errors. The mean absolute relative difference between the two methods was approximately 10%, with individual differences generally ranging from about 3% to 16%, which falls within the uncertainty commonly reported for chamber-based CO_2 flux measurements under field conditions.

Although the field comparison was not intended to represent a comprehensive intercomparison campaign covering all environmental conditions, the agreement observed over multiple measurement periods and a substantially broader flux range demonstrates that the laboratory-calibrated sensor performance can be effectively translated into field-based CO_2 flux measurements that agree with conventional manual

https://doi.org/10.5194/egusphere-2026-4934
Preprint. Discussion started: 21 September 2026

chamber observations. Together with the laboratory calibration results (Figure 6), these observations support the successful application of the integrated chamber design, gas circulation system, and flux calculation procedure to automated field-based CO_2 flux measurements.

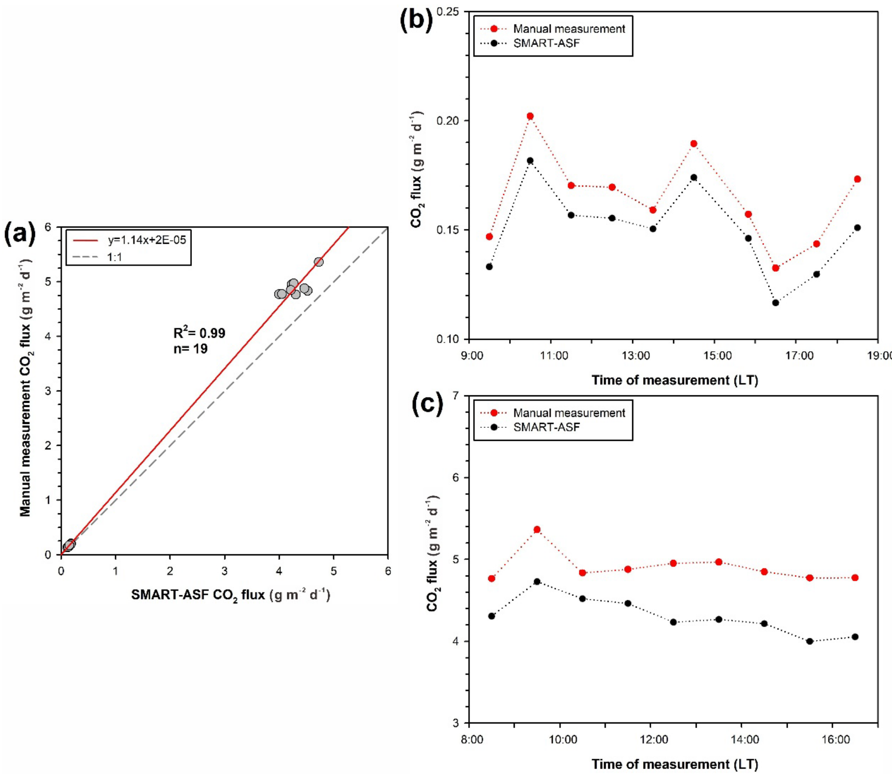

Figure 7. Field validation of the SMART-ASF system through comparison with conventional manual closed chamber measurements. (a) Relationship between paired CO_2 fluxes measured by the SMART-ASF system and the manual chamber method over a wide range of CO_2 fluxes (approximately 0.1–5.4 g m^{-2} d^{-1}). The dashed line represents the 1:1 relationship, and the solid red line indicates the linear regression (R^2 = 0.99, n = 19). (b) Time series comparison of paired CO_2 flux measurements under relatively low-flux conditions. (c) Time series comparison of paired CO_2 flux measurements under relatively high-flux conditions, demonstrating consistent agreement between the two methods across different emission levels.

https://doi.org/10.5194/egusphere-2026-4934
Preprint. Discussion started: 21 September 2026

3.2 Long-term field observations and operational performance

Long-term field observations were conducted from 8 September 2025 to 16 February 2026 to evaluate the long-term operational performance of the system under natural environmental conditions. Figure 8a presents the complete observation record, including time series of barometric pressure, chamber relative humidity and temperature, CO_2 concentration, calculated CO_2 flux, soil temperature at two depths (T_{S20} and T_{S100}), and precipitation. The precipitation data were obtained from a nearby Central Weather Administration meteorological station (C1AI50 Station; 25.0342° N, 121.6197° E), located approximately 2 km from the study site. Continuous observations were obtained throughout the deployment period.

The observation area was affected by a prolonged rainfall event associated with Typhoon Fengshen from 19 to 28 October 2025, as indicated by the precipitation peaks in Figure 8a. During this period, CO_2 flux declined from the previous range of approximately 0.1 to 1.4 g m^{-2} d^{-1} to values approaching background levels. This reduction is likely associated with heavy rainfall that temporarily filled soil pore spaces, restricted gas transport pathways, and reduced the effective diffusion of soil gases (Livingston et al., 2005; O'Connell et al., 2018). Despite the sustained reduction in solar radiation during this period, no interruption of system operation, wireless communication, or data transmission was observed.

To further illustrate the monitoring stability after the typhoon event, Figure 8b provides an enlarged view of the observation period from 1 November 2025 to 16 February 2026. During this interval, barometric pressure, chamber temperature and humidity, and CO_2 concentration exhibited short-term fluctuations driven by natural environmental variability, while CO_2 flux remained within a relatively stable low background range of approximately 0.01 to 0.2 g m^{-2} d^{-1}. In addition, soil temperatures at different depths displayed a typical seasonal cooling trend. The deeper soil temperature T_{S100} showed smaller variations and a slightly delayed response compared with T_{S20}, reflecting the effects of thermal diffusion and buffering within the soil profile (Holland et al., 1999).

Throughout the continuous deployment period of more than five months, no routine maintenance or component replacement was required. This operational experience suggests that the current system configuration is suitable for long-term deployment, particularly at remote or difficult-to-access monitoring sites where frequent maintenance is impractical.

https://doi.org/10.5194/egusphere-2026-4934
Preprint. Discussion started: 21 September 2026

Long-term observations during the stable background period from 1 November 2025 to 16 February 2026 (Figure 8b) yielded a mean CO_2 flux of 0.057 g m^{-2} d^{-1}, with a median of 0.053 g m^{-2} d^{-1} and a standard deviation of 0.035 g m^{-2} d^{-1}. These consistently low background fluxes indicate that CO_2 fluxes below 0.1 g m^{-2} d^{-1} can be resolved over extended observation periods. No obvious long-term drift was apparent in the field record, although a formal minimum detectable flux and periodic drift evaluation were not established in this study.

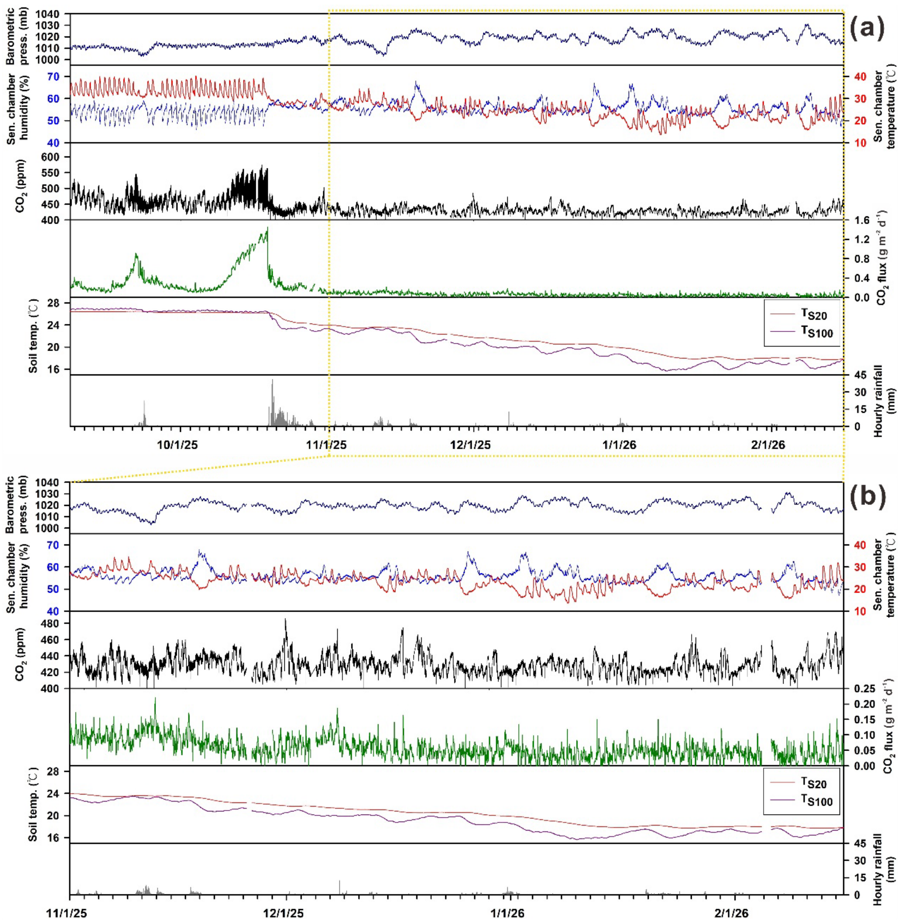

Figure 8. Long-term field observations recorded by the SMART-ASF system. (a) Complete dataset from 8 September 2025 to 16 February 2026, including barometric pressure, chamber relative humidity and temperature, CO_2 concentration, calculated CO_2 flux, soil temperature at depths of 20 cm and 100 cm, and hourly precipitation from a nearby meteorological station. The vertical dashed line indicates the period following a major rainfall event associated with Typhoon Fengshen. (b) Enlarged view

https://doi.org/10.5194/egusphere-2026-4934
Preprint. Discussion started: 21 September 2026

of the dataset from 1 November 2025 to 16 February 2026, showing background CO_2 flux variations and seasonal changes in soil temperature.

3.3 System versatility, limitations, and future applications

Beyond the successful validation of CO_2 flux measurements and long-term field operation, the SMART-ASF system was designed as a flexible monitoring platform that can be adapted to a broad range of environmental and geochemical applications. In the present study, CO_2 was selected as the principal target gas because the field deployment site was located in a non volcanic setting where sulfur bearing gases such as SO_2 and H_2S were expected to be negligible or below practical detection limits. Accordingly, system evaluation focused on CO_2 concentration dynamics and soil CO_2 flux performance. Nevertheless, SO_2 and H_2S sensing modules have already been integrated into the hardware architecture, and additional gas sensors can be incorporated according to site specific monitoring objectives. This modular configuration expands the potential applicability of the SMART-ASF platform beyond CO_2 only observations.

Such versatility is particularly relevant in environments where multi component gas emissions provide key information on subsurface processes. Potential applications include volcanic degassing, geothermal and hot spring systems, mud volcanoes, and fault related gas emissions, where sulfur species, carbon bearing gases, and other tracers may indicate fluid sources, permeability evolution, or hydrothermal activity (Chiodini et al., 2008; D'Alessandro et al., 2020; Kim et al., 2021; Li et al., 2024; Fu et al., 2025). In addition, the relatively low hardware cost of the SMART-ASF system enables denser spatial deployment than conventional commercial instruments, which is advantageous for resolving spatial heterogeneity in soil gas emissions and for establishing distributed monitoring arrays (Bastviken et al., 2015; Forbes et al., 2023). As summarized in Supplementary Table S1, the estimated material cost of one SMART-ASF unit is approximately USD 2,637 for the full multi gas configuration, including the autonomous solar powered energy supply module, but excluding labor, shipping, taxes, calibration gases, and server maintenance. Because the system can also be powered directly from mains electricity, the solar panel, battery, and charge controller are optional components and may be omitted where grid power is available. Furthermore, applications requiring only CO_2 monitoring do not require the SO_2 and H_2S sensor modules, further reducing the overall hardware cost. These configurable options allow the system to be adapted to autonomous remote deployments or fixed monitoring

https://doi.org/10.5194/egusphere-2026-4934
Preprint. Discussion started: 21 September 2026

stations and may facilitate denser multi-site deployment than conventional commercial systems.

In addition to its flexible and cost effective design, the SMART-ASF system incorporates several engineering features to minimize potential artifacts commonly associated with closed chamber measurements. One potential limitation of closed chamber techniques is that pressure buildup within the chamber may alter natural soil gas transport and introduce measurement artifacts (Pumpanen et al., 2004; Venterea and Baker, 2008). To minimize these effects, a one-way vent valve was incorporated into the chamber during both the accumulation and flushing stages to maintain chamber pressure close to ambient conditions. This configuration helps reduce pressure induced suppression of soil gas diffusion and minimizes feedback effects associated with progressive CO_2 accumulation within the chamber. Furthermore, the persistent near-linear increase in chamber CO_2 concentration throughout the selected flux calculation interval (Figure 3) suggests that pressure related disturbances and feedback effects were effectively minimized under the operating conditions adopted in this study.

Despite these advantages, several limitations should be considered. As with most low-cost sensor-based systems, long-term measurement quality depends on periodic calibration, environmental correction, and routine quality control. Previous studies have reported that low-cost NDIR CO_2 sensors are susceptible to zero drift and sensitivity changes associated with temperature, humidity, and sensor aging, while electrochemical gas sensors typically require periodic replacement during long-term operation (Brown et al., 2020; Macagga et al., 2024). While the SMART-ASF system incorporates temperature, humidity, and pressure monitoring together with a Nafion-based dehumidification module to reduce environmental interference, these design features reduce environmental influences on sensor performance under field conditions. Nevertheless, periodic calibration remains advisable during extended deployments to maintain measurement quality. Mechanical components and the autonomous power system also remain potential maintenance constraints, particularly at remote sites. Although no component replacement was required during the present five-month deployment, routine inspection of pumps, filters, tubing, batteries, and charging performance is recommended for longer deployments.

A further strength of the SMART-ASF system is its capacity for continuous high frequency observations combined with real time wireless data transmission and cloud-based visualization. This capability allows rapid detection of transient events, diurnal variability, and environmentally driven flux responses that are often undersampled by conventional manual chamber surveys, consistent with previous studies highlighting the advantages of automated chamber systems for capturing high temporal variability (Savage et al., 2014; Courtois et al., 2019; Themistokleous et al., 2024). Such measurements are particularly valuable for quantifying episodic rainfall effects, seasonal transitions, and short lived degassing anomalies associated with tectonic or hydrothermal processes.

The combination of low-cost sensing, modular architecture, and autonomous operation provides a practical framework for long-term soil gas monitoring. Future developments may include expanded multi gas capability, integration with meteorological and geophysical sensors, and deployment as dense observation networks for studies of soil carbon cycling, greenhouse gas exchange, volcanic unrest, and fluid migration along active fault systems.

4. Conclusions

This study presents the development and field validation of the low-cost SMART-ASF system for continuous soil gas flux monitoring. The system integrates automated chamber measurements, low-cost gas sensing, controlled circulation and flushing, wireless telemetry, and autonomous solar power. The principal conclusions are summarized as follows:

(1) Laboratory calibration and independent field validation demonstrated accurate automated CO_2 flux measurements over both laboratory and field conditions.

(2) Continuous field observations over more than five months documented uninterrupted acquisition of gas concentration, flux, meteorological, and soil temperature data under natural environmental conditions. Even during intense rainfall associated with Typhoon Fengshen, the SMART-ASF system operated without interruption in power supply, wireless communication, or data transmission. Furthermore, the system consistently resolved background CO_2 fluxes below 0.1 g m^{-2} d^{-1} during an extended period of stable field conditions, demonstrating sufficient sensitivity for long-term monitoring of low emission environments.

(3) High temporal resolution monitoring successfully captured short-term and seasonal variations in CO_2 flux associated with rainfall, soil temperature, and atmospheric variability. Heavy precipitation strongly suppressed fluxes, likely through temporary reduction of soil gas diffusivity caused by water filled pore space.

https://doi.org/10.5194/egusphere-2026-4934
Preprint. Discussion started: 21 September 2026

(4) The low-maintenance design, wireless data transmission, and expandable sensor architecture support deployment in distributed observation networks. Potential applications include soil carbon cycling, greenhouse gas monitoring, volcanic and fault-related degassing, and earthquake–fluid coupling studies.

Code and data availability

The laboratory calibration data, field validation datasets, representative long-term field observations, and data underlying the figures are available through Mendeley Data (Fu, 2026). The CO_2 flux calculation procedure is fully described in the manuscript and does not rely on proprietary data-processing software. The hardware architecture, system configuration, measurement workflow, and data-processing procedures are described in the manuscript and Supplementary Material to to enable reproduction of the methodology presented in this study.

Supplement

The supplement related to this article is available online and contains detailed hardware specifications, system configuration, component costs, and supplementary figures supporting the development and evaluation of the SMART-ASF system.

Author contributions

CCF conceived and supervised the study. CCF, LHL, and HKC contributed to the overall study design and scientific discussion. CCF and SFH designed and developed the experimental setup, sensor units, and data logging system, while LHL provided technical guidance throughout system development and laboratory evaluation. KHC conducted the laboratory calibration experiments. KHC and KWW participated in field deployment, manual chamber measurements, and field validation. CCF led the data analysis and interpretation with contributions from SFH and KHC. SFH developed the logger units and associated hardware described in the Supplementary Material. CSK developed the wireless data transmission and cloud-based visualization framework, and CJL contributed to the design and implementation of the power supply system. CCF and HKC acquired funding for this study. CCF prepared the original manuscript draft and led the writing and revision of the manuscript, with contributions from SFH, LHL, HKC, CSK, and CJL. All authors reviewed and approved the final manuscript.

Competing Interests

Author Sheng-Fu Hu was employed by the company XY ELECCONTROL TECHNOLOGY CO., LTD. The remaining authors declare that the research was conducted in the absence of any commercial or financial relationships that could be construed as a potential conflict of interest.

Acknowledgments

The authors gratefully acknowledge the field personnel for their support during instrument installation and field operations. Generative artificial intelligence (AI) tools were used solely to assist with English-language editing and grammar checking.

Financial support

This research was supported by the National Science and Technology Council (NSTC), Taiwan, under grant number NSTC 112-2740-M-001-001, NSTC 113-2116-M-001-017, NSTC 114-2119-M-002-033.

References

Aguilos, M., Hérault, B., Burban, B., Wagner, F., and Bonal, D.: What drives long-term variations in carbon flux and balance in a tropical rainforest in French Guiana?, Agr. Forest Meteorol., 253, 114–123, https://doi.org/10.1016/j.agrformet.2018.02.009, 2018.

Aubinet, M., Grelle, A., Ibrom, A., Rannik, Ü., Moncrieff, J., Foken, T., Kowalski, A. S., Martin, P. H., Berbigier, P., Bernhofer, C., Clement, R., Elbers, J., Granier, A., Grünwald, T., Morgenstern, K., Pilegaard, K., Rebmann, C., Snijders, W., Valentini, R., and Vesala, T.: Estimates of the annual net carbon and water exchange of forests: The EUROFLUX methodology, Adv. Ecol. Res., 30, 113–175, https://doi.org/10.1016/S0065-2504(08)60018-5, 1999.

Bastviken, D., Sundgren, I., Natchimuthu, S., Reyier, H., and Gålfalk, M.: Technical note: Cost-efficient approaches to measure carbon dioxide (CO_2) fluxes and concentrations in terrestrial and aquatic environments using mini loggers, Biogeosciences, 12, 3849–3859, https://doi.org/10.5194/bg-12-3849-2015, 2015.

Bastviken, D., Nygren, J., Schenk, J., Parellada Massana, R., and Duc, N. T.: Technical note: Facilitating the use of low-cost methane (CH_4) sensors in flux chambers – calibration, data processing, and an open-source make-it-yourself logger,

https://doi.org/10.5194/egusphere-2026-4934
Preprint. Discussion started: 21 September 2026

Biogeosciences, 17, 3659–3667, https://doi.org/10.5194/bg-17-3659-2020, 2020.

Blackstock, J. M., Covington, M. D., Perne, M., and Myre, J. M.: Monitoring atmospheric, soil, and dissolved CO_2 using a low-cost Arduino monitoring platform (CO_2-LAMP): Theory, fabrication, and operation, Front. Earth Sci., 7, 313, https://doi.org/10.3389/feart.2019.00313, 2019.

Brown, S. L., Goulsbra, C. S., Evans, M. G., Heath, T., and Shuttleworth, E.: Low cost CO_2 sensing: A simple microcontroller approach with calibration and field use, HardwareX, 8, e00136, https://doi.org/10.1016/j.ohx.2020.e00136, 2020.

Chiodini, G., Cioni, R., Guidi, M., Raco, B., and Marini, L.: Soil CO_2 flux measurements in volcanic and geothermal areas. Appl. Geochem., 13, 543-552, https://doi.org/10.1016/S0883-2927(97)00076-0, 1998.

Chiodini, G., Caliro, S., Cardellini, C., Avino, R., Granieri, D., and Schmidt, A.: Carbon isotopic composition of soil CO_2 efflux, a powerful method to discriminate different sources feeding soil CO_2 degassing in volcanic-hydrothermal areas, Earth Planet. Sci. Lett., 274, 372–379, https://doi.org/10.1016/j.epsl.2008.07.051, 2008.

Courtois, E. A., Stahl, C., Burban, B., Van den Berge, J., Berveiller, D., Bréchet, L., Soong, J. L., Arriga, N., Peñuelas, J., and Janssens, I. A.: Automatic high-frequency measurements of full soil greenhouse gas fluxes in a tropical forest, Biogeosciences, 16, 785–796, https://doi.org/10.5194/bg-16-785-2019, 2019.

D'Alessandro, W., Li Vigni, L., Gagliano, A. L., Calabrese, S., Kyriakopoulos, K., and Daskalopoulou, K.: CO_2 release to the atmosphere from thermal springs of Sperchios Basin and northern Euboea (Greece): The contribution of "hidden" degassing, Appl. Geochem., 119, 104660, https://doi.org/10.1016/j.apgeochem.2020.104660, 2020.

Forbes, E., Benenati, V., Frey, S., Hirsch, M., Koech, G., Lewin, G., Mantas, J. N., and Caylor, K.: Fluxbots: A method for building, deploying, collecting and analyzing data from an array of inexpensive, autonomous soil carbon flux chambers, J. Geophys. Res.-Biogeosci., 128, e2023JG007451, https://doi.org/10.1029/2023JG007451, 2023.

Fu, C. C., Yang, T. F., Tsai, M. C., Lee, L. C., Liu, T. K., Walia, V., Chen, C. H., Chang, W. Y., Kumar, A., and Lai, T. H.: Exploring the relationship between soil degassing and seismic activity by continuous radon monitoring in the Longitudinal Valley of eastern Taiwan, Chem. Geol., 469, 163–175, https://doi.org/10.1016/j.chemgeo.2016.12.042, 2017.

https://doi.org/10.5194/egusphere-2026-4934
Preprint. Discussion started: 21 September 2026

Fu, C. C., Mu, C. H., Kuo-Chen, H., Wang, P. L., Lin, L. H., Walia, V., Chen, K. H., and Wu, K. W.: Geochemical characteristics and origins of CO_2 emissions within the tectonic collision boundary of the Chihshang fault, eastern Taiwan, Geosci. Lett., 12, 23, https://doi.org/10.1186/s40562-025-00395-5, 2025.

Fu, C. C.: SMART-ASF: Development and field validation of a low-cost automated soil gas flux monitoring system for long-term field observations. [Dataset]. Mendeley Data V1. https://doi.org/10.17632/cbc52cnypg.1, 2026

Girault, F., Adhikari, L. B., France-Lanord, C., Agrinier, P., Koirala, B. P., Bhattarai, M., Mahat, S. S., Groppo, C., Rolfo, F., Bollinger, L., and Perrier, F.: Persistent CO_2 emissions and hydrothermal unrest following the 2015 earthquake in Nepal, Nat. Commun., 9, 2956, https://doi.org/10.1038/s41467-018-05138-z, 2018.

Holland, E. A., Robertson, G. P., Greenberg, J., Groffman, P., Boone, R., and Gosz, J.: Soil CO_2, N_2O, and CH_4 exchange, in: *Standard Soil Methods for Long-Term Ecological Research*, edited by: Robertson, G. P., Coleman, D. C., Bledsoe, C. S., and Sollins, P., Oxford University Press, New York, USA, 185–201, 1999.

Kim, C. Y., Yu, S., Oh, Y. Y., Chae, G., Yun, S. T., and Shinn, Y. J.: Short-term monitoring of geogenic soil CO_2 flux in a non-volcanic and seismically inactive emission site, South Korea, Front. Earth Sci., 8, 599388, https://doi.org/10.3389/feart.2020.599388, 2021.

Li, J., Guo, Z., Zhang, M., Zhao, W., Dingwell, D. B., Zheng, G., Sun, Y., and Cheng, Z.: Deep-sourced CO_2 emissions from the Eastern Himalaya Syntaxis and the Tengchong Volcanic Field, southeast Tibet, Chem. Geol., 645, 121888, https://doi.org/10.1016/j.chemgeo.2023.121888, 2024.

Livingston, G. P., Hutchinson, G. L., and Spartalian, K.: Diffusion theory improves chamber-based measurements of trace gas emissions, Geophys. Res. Lett., 32, L24817, https://doi.org/10.1029/2005GL024744, 2005.

Macagga, R., Asante, M., Sossa, G., Antonijevic, D., Dubbert, M., and Hoffmann, M.: Validation and field application of a low-cost device to measure CO_2 and evapotranspiration (ET) fluxes, Atmos. Meas. Tech., 17, 1317–1332, https://doi.org/10.5194/amt-17-1317-2024, 2024.

O'Connell, C. S., Ruan, L., and Silver, W. L.: Drought drives rapid shifts in tropical rainforest soil biogeochemistry and greenhouse gas emissions, Nat. Commun., 9, 1348, https://doi.org/10.1038/s41467-018-03352-3, 2018.

Pumpanen, J., Kolari, P., Ilvesniemi, H., Minkkinen, K., Vesala, T., Niinistö, S., Lohila,

https://doi.org/10.5194/egusphere-2026-4934
Preprint. Discussion started: 21 September 2026

A., Larmola, T., Morero, M., and Pihlatie, M.: Comparison of different chamber techniques for measuring soil CO_2 efflux, Agr. Forest Meteorol., 123, 159–176, https://doi.org/10.1016/j.agrformet.2003.12.001, 2004.

Savage, K., Phillips, R., and Davidson, E.: High temporal frequency measurements of greenhouse gas emissions from soils, Biogeosciences, 11, 2709–2720, https://doi.org/10.5194/bg-11-2709-2014, 2014.

Themistokleous, G., Savvides, A. M., Philippou, K., Ioannides, I. M., and Omirou, M.: A high-frequency greenhouse-gas flux analysis tool: Insights from automated non-steady-state transparent soil chambers, Eur. J. Soil Sci., 75, e13560, https://doi.org/10.1111/ejss.13560, 2024.

Tonolo, N., Cecconi, A., Vuth, S. M., Regine, M., Abruzzese, D., Carnevale, D., Bigi, A., Teggi, S., Bernardi, S., Bogliolo, M. P., and Verginelli, I.: Development of a novel low-cost automated flux chamber for real-time monitoring of VOC emissions at contaminated sites, Environ. Sci. Technol., 59, 8221–8230, https://doi.org/10.1021/acs.est.5c02365, 2025.

Venterea, R. T. and Baker, J. M.: Effects of soil physical nonuniformity on chamber-based gas flux estimates, Soil Sci. Soc. Am. J., 72, 1410–1417, https://doi.org/10.2136/sssaj2008.0019, 2008.

Werner, C., Kiese, R., and Butterbach-Bahl, K.: Soil–atmosphere exchange of N_2O, CH_4, and CO_2 and controlling environmental factors for tropical rain forest sites in western Kenya, J. Geophys. Res.-Atmos., 112, D03308, https://doi.org/10.1029/2006JD007388, 2007.

Yuce, G., Fu, C.-C., D'Alessandro, W., Gulbay, A. H., Lai, C.-W., Bellomo, S., Yang, T.-F., Italiano, F., and Walia, V.: Geochemical characteristics of soil radon and carbon dioxide within the Dead Sea Fault and Karasu Fault in the Amik Basin (Hatay), Turkey, Chem. Geol., 469, 129–146, https://doi.org/10.1016/j.chemgeo.2017.01.003, 2017.

Zawilski, B. M. and Bustillo, V.: Ultra-low-cost manual soil respiration chamber, Geosci. Instrum. Method. Data Syst., 13, 51–62, https://doi.org/10.5194/gi-13-51-2024, 2024.